Improvement of a Parallel Type Two-axial Actuator Controlled by a Multi-layered Neural Network

Kazuya Esumi, Masahiro Ohka*, Yasuhiro Sawamoto**, Shiho Matsukawa***, Tetsu Miyaoka****

*Department of Complex Systems Science, Graduate School of Information Science, Nagoya University, Furo-cho, Chikusa-ku, Nagoya, 464-8601

**Molex Co. , 1-5-4 Fukami Higashi, Yamato, 242-8585

***Olympus, Co., 2-3-1 Nishishinzyuku, Shinzyuku-ku, Tokyo 163-0914

**** Department Information System, Shizuoka Institute of Science and Technology, Toyosawa 2200-2, Fukuroi, 437-8555

Abstract:

Our parallel typed two-axial actuator was composed of two bimorph piezoelectric elements and two small links connected by three joints. We formulated kinematics for the parallel typed two-axial actuator because the endpoint is controlled in the two-dimensional coordinate. Since relationship between applied voltage and displacement cause by the voltage shows a hysteresis loop in the bimorph piezoelectric element used as components of the two-axial actuator, we produce a control system for the two-axial actuator based on a multi-layered artificial neural network to compensate the hysteresis. The neural network is comprised of 4 neurons in the input layer, 10 neurons in the hidden layer and ones neuron in the output layer. The output neuron emits time derivative of voltage; two bits signal expressing increment or decrement condition is generated by two input neurons; one of the other two input neurons and the other calculate current values of voltage and displacement, respectively. In the learning process, the network learns the hysteresis including minor loops. In the verification test, the endpoint of the two-axial actuator traces the desired circular trajectory in the two-dimensional coordinate system. After learning hysteresis loops including minor loops, the neural network simulates these hysteresis phenomena with very high accuracy.

1. INTRODUCTION

Simultaneous presentation of pressure distribution and shearing force is effective to enhance presentation reality of a tactile display[1]-[7] because there are pressure and shearing force accepting points (mechanoreceptive units) distributing on human palm and finger surfaces[8][9]. Thus, we are studying a two-axial micro-actuator[10][11] for development of a tactile display pad of two-axial actuators.

Our parallel typed two-axial actuator was composed of two bimorph piezoelectric elements and two small links connected by three joints. We formulated kinematics for it due to two-dimensional control of its endpoint (movable end, hereafter) in the two-dimensional coordinate system. The movable end of the two-axial actuator does not follow same route in increment and decrement of applied voltage because the present two-axial actuator utilizes piezoelectric elements possessing a hysteresis phenomenon.

In the previous study, a new control method for the piezoelectric actuator is established on the basis of a multi-layered artificial neural network [12]-[14] to achieve the sensor-less control of the actuator. Since the network scale becomes huger without a new idea to learn the hysteresis loop, we apply causality to formulate the modified neural network. In the causality which is a basic idea of the classical physics, a certain current time derivative of physical variable is determined by current physical variables if all physical variables can be measured at a certain instant. On the basis of the causality, we assumed that the current time increment of the voltage is determined by the current voltage, the current displacement and flags indicating increment or decrement condition. The present network is comprised of 4 neurons in the input layer, 10 neurons in the hidden layer and one neuron in the output layer. The current values of voltage and displacement are input to the two of the 4 neurons in the input layer; two bits signal expressing increment or decrement condition calculated from time derivative of displacement are input to the other two neurons; the output neuron emits time derivative of voltage. After time integration operation is performed to the output, the integrated output is used as voltage value, which should be applied to the actuator. Simultaneously, the voltage is applied to the input neuron as feedback signal. Although in the other researcher's study the idea of using the neural network has been also used to control the piezoelectric actuator [15], it is noted that the integration operation is included in the abovementioned feedback loop to reduce the network scale.

In this study, both of hardware and software are improved on the basis of the previous study[16]. Although the movable joint of the two-axial actuator roughly traced the desired circular trajectory in the two-dimensional coordinate system, the movable joint was apart from the desired trajectory in the last half. This is caused by loose fitting between the pin and hole, which play as a role of a joint. We designed and developed a revised version of the

978-1-4244-2919-6/08/$25.00 ©2008 IEEE

two-axial micro actuator using a micro sliding bearing. 4. Additionally, learning procedure of the multi-layered neural network was improved by adding some minor loops to leaning data. The abovementioned improvements are continued at the present. In the conference, we will show these results.

2. Two-axial Actuator

2.1 Kinematics of Parallel Type Two-axial Actuator

Figure 1 shows mechanism and photograph of the two-axial actuator, respectively. It is composed of two piezoelectric elements, three joints and two small links to generate two-dimensional displacement as shown in Fig. 1. The displacement of movable end (the center joint C) is controlled by controlling the displacement of right and left bimorph type piezoelectric elements. First, to formulate kinematic equation of the two-axial actuator, nomenclatures used in the formulation are shown as follows:

a : length of the small link.
b : distance between joint A and B in reference configuration.
u_x : x-directional displacement of movable end C.
u_y : y-directional displacement of movable end C.
u_R : bending displacement of right piezoelectric element.
u_L : bending displacement of left piezoelectric element.
V_R : applied voltage of right piezoelectric element.
V_L : applied voltage of left piezoelectric element.
θ : establishment angle of piezoelectric element.
$\dot{x}$: the time derivative of the variable x.

Coordinates of points A' and B' are calculated from geometrical relationship shown in Fig 1 as follows. That is,

Point A': $\left(-\frac{1}{2}b+u_L\sin\theta,\ \sqrt{a^2-\frac{b^2}{4}}-u_L\cos\theta\right)$

Point B': $\left(\frac{1}{2}b-u_R\sin\theta,\ \sqrt{a^2-\frac{b^2}{4}}-u_R\cos\theta\right)$

where, $a > b/2$.

When the vector of movable end is expressed as $\mathbf{u}=u_x\mathbf{i}+u_y\mathbf{j}$, the following expressions are obtained from the condition of link length being constant.

$$\left(u_x+\frac{1}{2}b-u_L\sin\theta\right)^2+\left(u_y-\sqrt{a^2-\frac{b^2}{4}}+u_L\cos\theta\right)^2=a^2 \quad \text{(1)}$$

$$\left(u_x-\frac{1}{2}b+u_R\sin\theta\right)^2+\left(u_y-\sqrt{a^2-\frac{b^2}{4}}+u_R\cos\theta\right)^2=a^2 \quad \text{(2)}$$

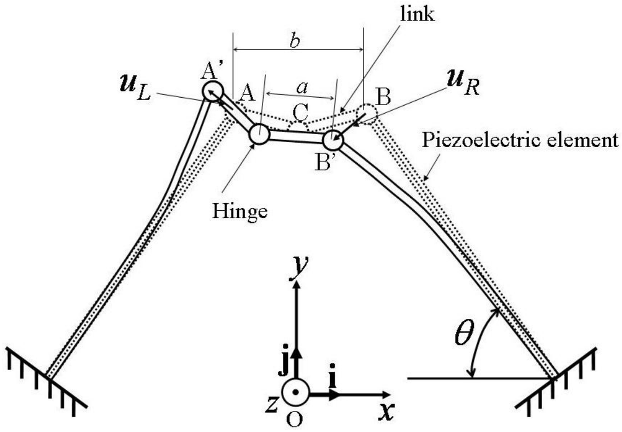

Fig. 1 Principle of the parallel typed two-axial actuator

The following equations are obtained from differentiating Eq.(1) and (2).

$$2\left(u_x+\frac{1}{2}b-u_L\sin\theta\right)\left(\dot{u}_x-\dot{u}_L\sin\theta\right)+2\left(u_y-\sqrt{a^2-\frac{b^2}{4}}+u_L\cos\theta\right)\left(\dot{u}_y+\dot{u}_L\cos\theta\right)=0 \quad \text{(3)}$$

$$2\left(u_x-\frac{1}{2}b+u_R\sin\theta\right)\left(\dot{u}_x+\dot{u}_R\sin\theta\right)+2\left(u_y-\sqrt{a^2-\frac{b^2}{4}}+u_R\cos\theta\right)\left(\dot{u}_y+\dot{u}_R\cos\theta\right)=0 \quad \text{(4)}$$

Simultaneous equation composed of Eq.(3) and (4) is written as following matrix expression:

$$\begin{pmatrix}\dot{u}_L\\ \dot{u}_R\end{pmatrix}=\begin{bmatrix}\frac{A_{11}}{A_{11}\sin\theta-A_{12}\cos\theta} & \frac{A_{12}}{A_{11}\sin\theta-A_{12}\cos\theta}\\ -\frac{A_{21}}{A_{21}\sin\theta+A_{22}\cos\theta} & -\frac{A_{22}}{A_{21}\sin\theta+A_{22}\cos\theta}\end{bmatrix}\begin{pmatrix}\dot{u}_x\\ \dot{u}_y\end{pmatrix} \quad \text{(5)}$$

$$A_{11}=u_x+\frac{1}{2}b-u_L\sin\theta \quad \text{(6)}$$

$$A_{12}=u_y-\sqrt{a^2-\frac{b^2}{4}}+u_L\cos\theta \quad \text{(7)}$$

$$A_{21}=u_x-\frac{1}{2}b+u_R\sin\theta \quad \text{(8)}$$

$$A_{22}=u_y-\sqrt{a^2-\frac{b^2}{4}}+u_R\cos\theta \quad \text{(9)}$$

2.2 Neural Network Including Feedback Loop

In the present research, we are attempting to achieve the sensor-less control of the actuator, which is established by a new control method of piezoelectric actuator using a neural network model. The present structure of network is featured with causality as a basic idea, in which time increment of

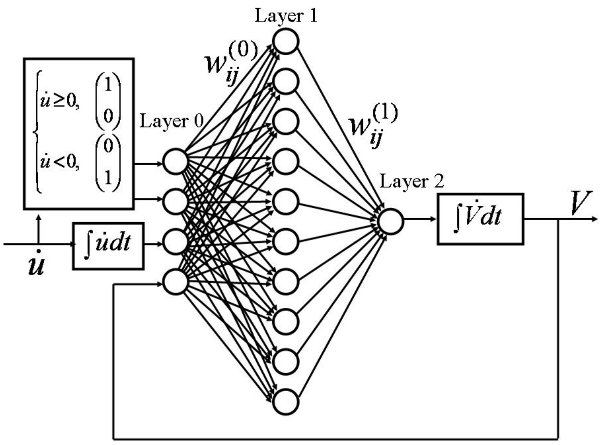

Fig.2 Neural network with a feedback loop

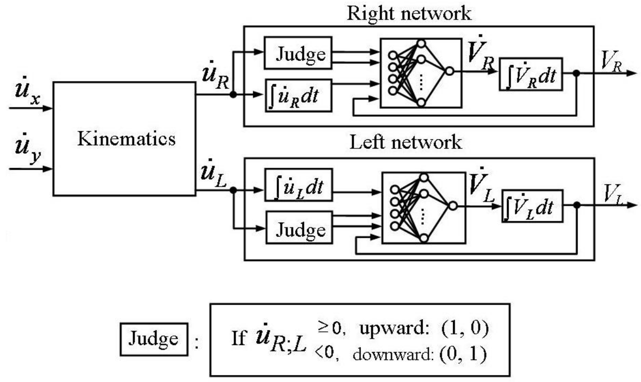

Fig. 3 Block diagram for controller equipped with neural networks

physical variable is determined at a certain instant, if all current physical variables can be measured at the moment.

Generally, it is well known that in piezoelectric actuator slope of the voltage-displacement curve is different noticeably between increment and decrement sequences of applied voltage. If the above-mentioned causality is applied to control method of piezoelectric actuator, the time increment of voltage at a certain instant can be determined by current voltage, current displacement and information related to whether increment or decrement condition.

Figure 2 shows structure of the present neural network; it is comprised of 4 neurons in the input layer, 10 neurons in the hidden layer and one neuron in the output layer. The output neuron emits time derivative of voltage; two bits signal expressing increment or decrement condition is generated by two input neurons; one of the other two input neurons and the other show current values of voltage and displacement, respectively. After time integration the output time derivative of displacement is not only used for voltage that should be applied to piezoelectric element, but also fed to the neuron in the input layer through a feedback loop. The neural network is featured with the feedback loop including an integral unit to reduce number of neurons.

In the learning process, synaptic connection's weight $w_{ij}^{(s)}$ is adjusted by using the back propagation algorithm for neural networks after the feedback loop shown in Fig.3 is removed. Where, the suffix s shows layers and s = 0 and 1 are input layer to the hidden layer and the hidden layer to the output layer, respectively. The suffix i and j denote the neurons number and depend on layer; if s = 0, then i = 0,1,2,3 and j = 0,1, …,9; if s = 1, then i= 0,1, …,9 and j = 0. Since the error back propagating method to adjust synaptic connection's weight is introduced at many other references [12]-[14], expressions related to it are abbreviated in the present paper.

Voltage history including increment and decrement process is applied to piezoelectric element to obtain data for network learning. In the network learning, we used data composed of about one hundred patterns of two bits expressing increment or decrement, applied voltage, displacement and displacement derivative *dV/du* of voltage. Therefore, the value of displacement derivative *dV/du* of voltage will be output from the output neuron. Since *du/dt* is given from the trajectory planning, the time derivative of voltage is calculated by multiplying *du/dt* by *dV/du*.

In addition, usual error back propagation is applicable to the present neural network with removing the feedback loop from the present network. This is different from the RTRL [15] of recurrent neural networks.

2.3 Control System

In the present two-axial actuator, the positional error will be caused by individual differences about not only the inclination of a linear portion in the hysteresis loop but also non-linearity and width of the loop. The influence of the individual difference is modified by individually putting in the characteristic of right and left actuators according to the neural network model.

Figure 3 shows block diagram of the control system designed on the basis of the above-mentioned idea. The neural network is incorporated into this control system to control right and left piezoelectric elements.

At first, $\dot{u}_x$ and $\dot{u}_y$ are decided from designed trajectory in two-dimensional area. The displacement rates of right and left type piezoelectric elements $\dot{u}_L$ and $\dot{u}_R$

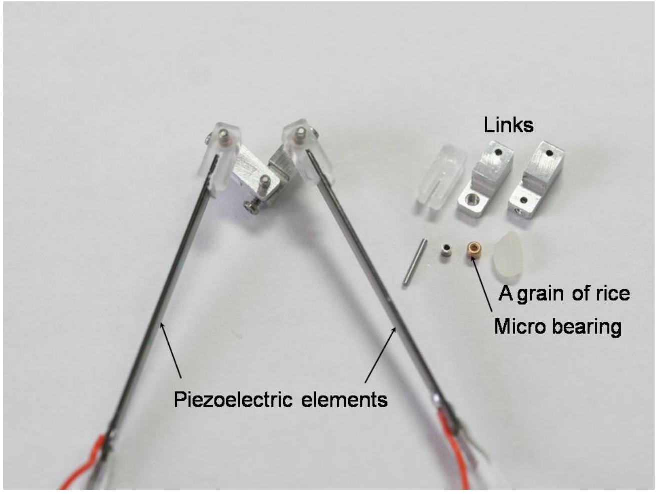

Fig. 4 Newly designed and developed new 2D micro actuator and mechanical elements (the left panel shows the 2D micro actuator; a grain of rice displayed for comparison)

are calculated by substituting $\dot{u}_x$ and $\dot{u}_y$ into the kinematic equation Eq. (5). Then, u_L and u_R is obtained by numerical integral of $\dot{u}_L$ and $\dot{u}_R$.
The 0th and the 1st neurons of right and left neural networks in the input layer accept binary number 1 or 0 judging increment or decrement condition. The condition of increment or decrement is simply decided according to sign of $\dot{u}_L$ and $\dot{u}_R$. If the sign is positive or negative, the judgment is increment or decrement. For example, if the input vector of the left piezoelectric element is $(1 \quad 0 \quad u_L \quad V_L)^T$ or $(0 \quad 1 \quad u_L \quad V_L)^T$, the condition is specified as increment or decrement.

Since the displacement derivative of the voltage is output from the output neuron of the neural network as previously mentioned, the time derivative of voltage is calculated by multiplying the time derivative of displacement by it. In addition, after integration the voltage is applied to the piezoelectric element, and is fed to the input layer through the feedback loop.

3. Experimental Procedure

3.1 Prototype of the Two-Axial Actuator

The parallel typed two-axial actuator is comprised of two bimorph type piezoelectric elements, two small links and three joints as shown previously in Fig. 4. The piezoelectric element (length: 31mm, width: 2.0mm, thickness: 0.50mm) is disassembled from Braille cell SC9[5], which has been developed for the visually handicapped person by KGS Ltd. The small links of 5mm in length made of aluminum alloy are used in this actuator.

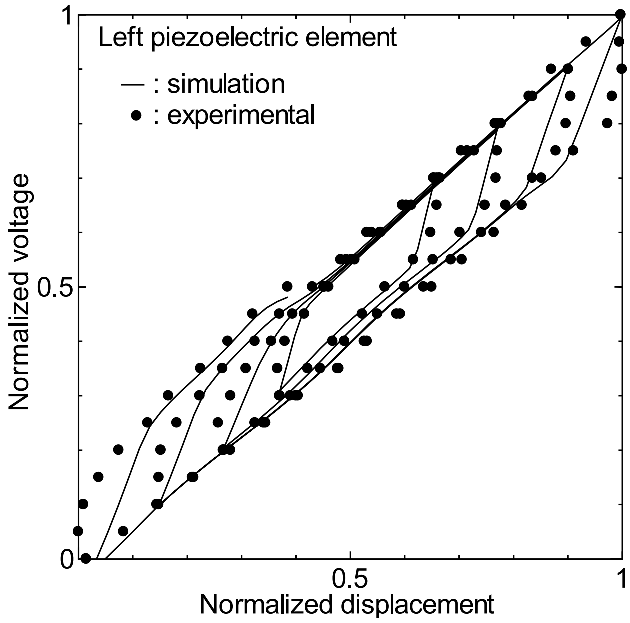

Fig. 5 Simulated result of left piezoelectric element

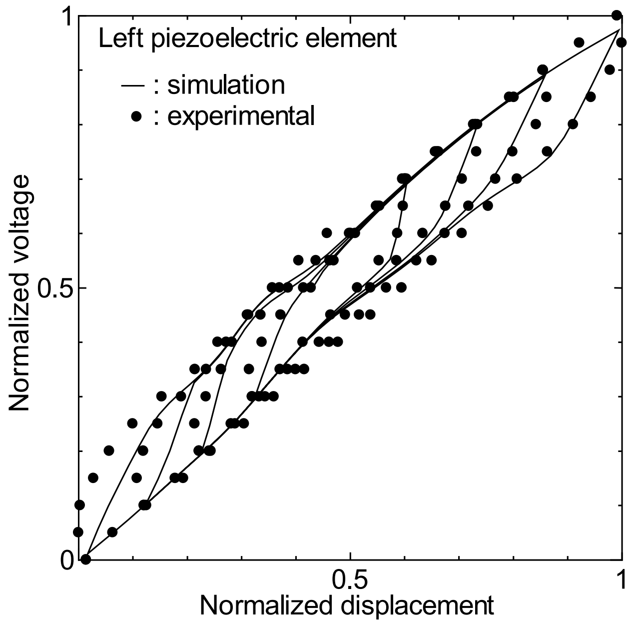

Fig. 5 Simulated result of right piezoelectric element

Since the two links or the link and the piezoelectric element end are connected with a joint of the aluminum alloy, they are able to rotate mutually. The center of the three joints was functioned as the movable end. In these joints, micro sliding bearings are used to remove gap between shaft and bearing. The bearing has the same size of rice grain as shown in Fig. 4.

3.2 Evaluation Apparatus

We used a microscope (OLYMPUS, inverted research microscope: IX71) for measures displacements of the three joints. The 1.25-power PlanApo×1.25 for objective lens and the 0.35-power U-TV0.35×C-2 for a camera adaptor were used. The movement trajectories of joint A, B and C were measured by image data processing of image retrieved by a CCD camera mounted in the microscope. In the image data processing, centroid coordinates of these joints were obtained with noise reduction and circular regression. The above-mentioned operation was executed in each stepwise voltage variation to measure trajectories of the three joints. Multifunctional universal image analysis software (Library Ltd., cosmos 32 Ver4.6) was used for the image processing.

3.3 Experimental Procedure

In order to adjust weight $w_{ij}^{(s)}$ of synaptic connection, the following experiment was performed. This experiment is performed to examine the relationship between applied voltage and displacements of right and left piezoelectric elements. In this experiment, 100V datum voltage was applied to right and left piezoelectric elements at first and it was made a starting point. In discussion in the subsequent sections, the voltage 100V will be expressed as 0V. In the beginning the voltage is sequentially increased to 40V at intervals of 10V, and then the applied voltage is decreased to -40 V at intervals of 10V. Subsequently, it is decreased to -60V after increased to 60V at intervals of 10V; it is decreased to -80V after increased to 80V at intervals of 10V; it is decreased to -100V after increased to 100V at intervals of 10V. In addition, it is increased to the starting point 0V at intervals of 10V. Centroid displacements of joint A, B and C were measured at every stepwise variation.

4. EXPERIMENTAL RESULT AND DISCUSSION

Hysteresis loops of the left piezoelectric element obtained by the present experiment are shown in Fig. 5 by ●. The solid line in Fig. 5 is output result of the control system shown in Fig. 3. The output result from the neural network almost coincides with the experimental result for not only a large loop of ±100 V but also a small inside loops of ±40, ±60 and ±80 V.

Next, hysteresis loops of the right piezoelectric element obtained by the present experiment are shown in Fig. 6 by ●. The solid line in Fig. 6 is output result of the control system. Inclination of the right element is the same as that of the left element. The output result from the neural network almost coincides with the experimental result. Therefore, the high accuracy learning result is obtained as abovementioned.

If the result of left piezoelectric element is compared to that of right element, we can notice that displacement amplitudes and the inclinations coincide on right and left piezoelectric elements. Although precise hysteresis characteristics such as the loop width are considerably different, the present neural system can follow the sight difference.

In addition, 100 thousand times of iteration was needed to obtain the learning result of Fig.6. The calculation was executed on a notebook computer (Panasonic, CF-R4), and required about 15 minutes to complete the learning calculation.

5. CONCLUSION

The control method of two-axial actuator was presented to enhance positioning accuracy and to apply it to the tactile display. In order to realize sensor-less control of piezoelectric actuators possessing obvious hysteresis characteristic, we established a new neural network model including feedback loop based on causality that the time derivative of applied voltage was determined by increment or decrement condition, current voltage and displacement.

The two-axial micro actuator was composed of the right and left bimorph piezoelectric elements, two links and three joints. The control system was also developed with incorporating the neural network for compensation of the hysteresis characteristic.

The learning was terminated within reasonable calculation time; after the learning process, it was able to reproduce hysteresis characteristics including several minor loops in high accuracy.

In the future, it is necessary to enhance accuracy of in software with increasing number of learning data and accuracy joint bearings with exchanging the present hand-made one for precise one.

ACKNOWLEDGEMENT

This study was supported by fiscal 2008 grants from the Ministry of Education, Culture, Sports, Science and Technology (Grant-in-Aid for Scientific Research in Priority Areas, No. 1607807)

REFERENCES

[1] Y. Ikei, M. Yamada, and S. Fukuda: Tactile Texture Presentation by Vibratory Pin Arrays Based on Surface Height Maps, Proc. of Int. Mechanical Engineering Conf. and Exposition, (1999), 51-58.

[2] M. Takahashi, T. Nara, S. Tachi, and T. Higuchi: A Tactile Display Using Surface Acoustic Wave, Proc. of the 2000 IEEE Inter. Workshop on Robot and Human Interactive Communication, (2000), 364-367.

[3] Y. Tanaka, H. Yamauchi, and K. Amemiya: Wearable Haptic Display for Immersive Virtual Environment, Fifth JFPS Inter. Symposium, (2002), 309-310.
[4] PHANToM, http://www.sensable.com/products/phantom_ghost
[5] Braille Cells, http://www.kgs-jpn.co.jp/epiezo.html
[6] M. Ohka, K. Kato, T. Fujiwara, and Y. Mitsuya: Virtual Object Handling Using a Tactile-haptic Display System, The Inter. Conf. on Mechatronics and Automation, (2005), 292-297.
[7]M. Ohka, H. Koga: Y. Mouri, T. Sugiura, T. Miyaoka and Y. Mitsuya, Figure and Texture Presentation Capabilities of a Tactile Mouse Equipped with a Display Pad of Stimulus Pins, Robotica, Vol. 25, (2007), pp. 451-460.
[8] T. Miyaoka: Measurements of detection thresholds presenting normal and tangential vibrations on human glabrous skin, Proceedings of the Twentieth Annual Meeting of the International Society for Psychophysics, Vol. 20, (2004), 465-470.
[9] T. Miyaoka: Mechanoreceptive mechanisms to determine the shape of the detection-threshold curve presenting tangential vibrations on human glabrous skin, Proceedings of the 21st Annual Meeting of The International Society for Psychophysics, Vol. 21 (2005), 211-216.
[10]M. Ohka, S. Matsukawa, Y. Sawamoto, T. Miyaoka and Y. Mitsuya: A Two-axis Bimorph Piezoelectric Actuator Controlled by a Multi-layered Neural Network, Proc. of Actuator 2006, 10^{th} Inter. Conf. on New Actuator, (2006), pp. 503-506.
[11] M. Ohka: Tactile display, multi-axial actuator, and manipulation equipment, Patent submit number: 2006-081528.
[12] D. E. Rumelhart, G. E. Hinton and R.J. Williams, "Learning Representations by Back-propagating Errors, Nature, Vol. 323-9, (1986), pp. 533-536.
[13]Satish Kumar: Neural Networks, McGrow-Hill, (2005).
[14]R. Williams and D. Zipser: A Learning Algorithm for Continually Running Fully Recurrent Neural Networks, Neural Computation, Vol. 1, (1989), pp. 270-280.
[15]S. Yu, G. Alici and B. Shirnzadeh: Modeling Rate-dependent Hysteresis in Piezoelectric Actuators with Neural Networks, Eighth Inter. Conf. on Proc. of Manufacturing Management, (2004), pp. 826-833.
[16] M. Ohka, Y. Sawamoto, S, Matsukawa, T. Miyaoka and Y. Mitsuya, Parallel Type Two-axial Actuator Controlled by a Multi-layered neural Network, Proc. of the 2007 Inter. Sympo. On Micro-NanoMechatronics and Human Science (MHS2007 Micro-Nano COE), (2007), pp. 418-423.